Dedicated to innovation in aerospace

NLR-TP-2016-360 | March 2017

The Scattering of Open Rotor Tones by a Cylindrical Fuselage and its Boundary Layer

CUSTOMER: Netherlands Aerospace Centre

NLR – Netherlands Aerospace Centre

Netherlands Aerospace Centre

NLR is a leading international research centre for aerospace. Bolstered by its multidisciplinary expertise and unrivalled research facilities, NLR provides innovative and integral solutions for the complex challenges in the aerospace sector.

NLR's activities span the full spectrum of Research Development Test & Evaluation (RDT & E). Given NLR's specialist knowledge and facilities, companies turn to NLR for validation, verification, qualification, simulation and evaluation. NLR thereby bridges the gap between research and practical applications, while working for both government and industry at home and abroad.

NLR stands for practical and innovative solutions, technical expertise and a long-term design vision. This allows NLR's cutting edge technology to find its way into successful aerospace programs of OEMs, including Airbus, Embraer and Pilatus. NLR contributes to (military) programs, such as ESA's IXV re-entry vehicle, the F-35, the Apache helicopter, and European programs, including SESAR and Clean Sky 2.

Founded in 1919, and employing some 650 people, NLR achieved a turnover of 71 million euros in 2016, of which three-quarters derived from contract research, and the remaining from government funds.

For more information visit: **www.nlr.nl**

Dedicated to innovation in aerospace

EXECUTIVE SUMMARY

UNCLASSIFIED

The Scattering of Open Rotor Tones by a Cylindrical Fuselage and its Boundary Layer

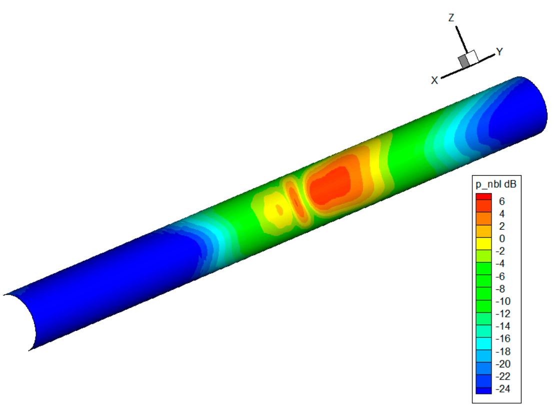

REPORT NUMBER
NLR-TP-2016-360

AUTHOR(S)
H.H. Brouwer

REPORT CLASSIFICATION
UNCLASSIFIED

DATE
March 2017

KNOWLEDGE AREA(S)
Aeroacoustic and Experimental Aerodynamics

DESCRIPTOR(S)
Aircraft Noise
Open rotors

Problem area

Because of the increasing interest in fuel-efficient aircraft, the application of open rotors is actively being researched as an alternative propulsion system for airliners. Both single-rotating and contra-rotating open rotors have gained renewed interest, because of practically unlimited bypass ratio's. One of the issues of open rotors is the noise level, both external and inside the cabin. The use of advanced CFD/CAA methods, as well as extensive wind tunnel testing, has produced a lot of knowledge on the noise generated by these propulsion systems. However, the computation (or measurement) of the sound field of a complete aircraft model with rotating open rotors is still very costly, much more costly than the assessment of the noise from an isolated propulsion system. Therefore the need exists for fast computation models for the installation effects on the noise of an open rotor.

Description of work

An analytical method has been developed for the acoustic interaction of open rotors and a cylindrical fuselage including its boundary layer. The source is represented by a proven lifting-line model in the case of single-rotation propeller

(SR). In the case of a contra-rotating open rotor (CROR) the source is modelled by a similar model, which does not represent a CROR in full detail, but has the physically correct radiation properties.
The fuselage is modelled as a circular cylinder, embedded in a uniform flow, parallel to its axis. The effect of a boundary layer is included. A number of examples has been analyzed, pertaining to the scattering of rotor-alone tones and CROR interaction tones. Results have been computed for the acoustic pressure on the fuselage, relevant for cabin noise, and the acoustic pressure in the far field, relevant for the impact on the environment.

Results and conclusions

A analytical method has been obtained for the computation of the acoustic interaction of open rotors and a rigid cylinder, representing an aircraft fuselage. In the computation of the sound field of an installed configuration the boundary layer can be incorporated. The model is suitable for computing both the acoustic pressure on the fuselage wall, relevant for cabin environment studies, and the pressure waves radiated to the far-field. The effort to prepare the computations and the computational costs are very low.

Applicability

The analytic formulations presented in this report provide a powerful tool to estimate the effect of a fuselage and it boundary layer on rotor noise, both as it impinges on the fuselage itself and as it radiates to the far field. Although the method is not suitable to predict installed rotor noise accurately for a real aircraft geometry, it can be used to better understand the effects, to yield a quick first estimate of the installation effects, and to serve as a benchmark for high-fidelity computational methods.

GENERAL NOTE
This report is based on a presentation held at the 22nd AIAA/CEAS Aeroacoustics Conference, Lyon, France, 30 May - 1 June, 2016.

NLR
Anthony Fokkerweg 2
1059 CM Amsterdam
p) +31 88 511 3113 f) +31 88 511 3210
e) info@nlr.nl i) www.nlr.nl

Dedicated to innovation in aerospace

NLR-TP-2016-360 | March 2017

The Scattering of Open Rotor Tones by a Cylindrical Fuselage and its Boundary Layer

CUSTOMER: Netherlands Aerospace Centre

AUTHOR(S):

H.H. Brouwer NLR

NLR - Netherlands Aerospace Centre

This report is based on a presentation held at the 22nd AIAA/CEAS Aeroacoustics Conference, Lyon, France, 30 May - 1 June, 2016.

CUSTOMER	**Netherlands Aerospace Centre**
CONTRACT NUMBER	**- - -**
OWNER	**Netherlands Aerospace Centre**
DIVISION NLR	**Aerospace Vehicles**
DISTRIBUTION	**Unlimited**
CLASSIFICATION OF TITLE	**UNCLASSIFIED**

APPROVED BY :		
AUTHOR	**REVIEWER**	**MANAGING DEPARTMENT**
H.H. Brouwer	K. Lammers	J.F. Hakkaart
DATE 10 04 17	DATE 03 05 17	DATE 10 04 17

Contents

This page is intentionally left blank.

The Scattering of Open Rotor Tones by a Cylindrical Fuselage and its Boundary Layer

Harry H. Brouwer[1]

Netherlands Aerospace Centre NLR, 1006 BM Amsterdam,The Netherlands

A method is presented for the acoustic interaction of open rotors and a cylindrical fuselage including its boundary layer. The source is represented by a proven lifting-line model in the case of single-rotation propeller (SR). In the case of a contra-rotating open rotor (CROR) the source is modelled by a similar model, which does not represent a CROR in full detail, but has the physically correct radiation properties. The fuselage is modelled as a circular cylinder, embedded in a uniform flow, parallel to its axis. The effect of a boundary layer is included. The mathematical model of both the sources and the scattering is given. Numerical results are presented for both a single-rotation propeller and a CROR, in terms of the acoustic pressure on the fuselage, and in the far field. Directivity plots show interference patterns with a strong variation of the sound pressure level as a function of circumferential angle. At larger distances the results are distorted by the discrete Fourier transformation, if applied to the same axial domain. This might be solved by the use of a large computational domain, especially in the case of interaction tones, which radiate over a wider angular range than rotor-alone tones. As an alternative, an asymptotic approximation is derived for large distances, avoiding the discrete Fourier transformation. The analytic formulations presented in this paper provide a powerful tool to estimate the effect of a fuselage and its boundary layer on rotor noise, both as it impinges on the fuselage itself and as it radiates to the far field. The method can be used to yield a quick first estimate of the installation effects, and to serve as a benchmark for high-fidelity computational methods.

Nomenclature

A_n	=	coefficient of reflected acoustic pressure
α	=	axial wavenumber
B	=	blade number
B_F	=	blade number front rotor
B_R	=	blade number rear rotor
B_n	=	multiplication factor for acoustic pressure in boundary layer
β	=	$\sqrt{1-M^2}$
g	=	generic function
γ	=	radial wavenumber
$\bar{\bar{D}}$	=	tensor representing thickness and moment in lifting-line source
$\vec{L}$	=	lift
M	=	flight Mach number
p	=	acoustic pressure
p_b	=	acoustic pressure in the boundary layer
p_{tot}	=	total acoustic pressure
p_{re}	=	reflected acoustic pressure
p_{in}	=	incoming acoustic pressure
$\hat{p}_n$	=	circumferential component of acoustic pressure

[1] Senior Scientist, Department of Helicopters and Aeroacoustics, P.O. Box 90502.

$\tilde{p}_n$	=	axial Fourier transform of $\hat{p}_n$
$\tilde{Q}_{n,m}$	=	modal CROR source strength
$\vec{q}$	=	vector representing unsteady lift
R	=	$\sqrt{\left(\frac{x}{\beta}\right)^2 + r^2}$
R_f	=	radius of fuselage
r	=	radial coordinate
r_p	=	radial coordinate in rotor reference system
r_h	=	dimensionless hub radius
t	=	time
U	=	relative flow velocity at blade section
θ	=	angular coordinate
θ_p	=	angular coordinate in rotor reference system
x	=	axial coordinate
φ	=	polar angle in $(x/\beta, r)$ plane
Ω	=	angular velocity
Ω_F	=	angular velocity front rotor
Ω_R	=	angular velocity rear rotor
ω	=	angular frequency

I. Introduction

BECAUSE of the increasing interest in fuel-efficient aircraft, the application of open rotors is actively being researched as an alternative propulsion system for airliners. Both single-rotating and contra-rotating open rotors have gained renewed interest, because of practically unlimited bypass ratio's. One of the issues of open rotors is the noise level, both external and inside the cabin. The use of advanced CFD/CAA methods, as well as extensive wind tunnel testing, has produced a lot of knowledge on the noise generated by these propulsion systems. However, the computation (or measurement) of the sound field of a complete aircraft model with rotating open rotors is still very costly, much more costly than the assessment of the noise from an isolated propulsion system. Therefore the need exists for fast computation models for the installation effects on the noise of an open rotor. An example of such a model is presented in references 1 and 2, where an analytic model is presented for the acoustic interaction of rotating point sources and rigid surfaces, such as a cylinder.

In this paper a method is presented for the acoustic interaction of open rotors and a cylindrical fuselage including its boundary layer. The source is represented by a proven lifting-line model in the case of single-rotation propeller (SR). In the case of a contra-rotating open rotor (CROR) the source is modelled by a similar model, which does not represent a CROR in full detail, but has the physically correct radiation properties.

The fuselage is modelled as a circular cylinder, embedded in a uniform flow, parallel to its axis. The effect of a boundary layer is included. In the first sections of the paper the mathematical model is given. Then results will be presented for both a single-rotation propeller and a CROR, in terms of the acoustic pressure on the fuselage, and in the far field. Finally, an asymptotic approximation is derived for the acoustic pressure in the very far field.

II. General model description

The model problem consists of an infinitely long cylindrical fuselage and a rotor, which can be either a single rotation rotor or a contra-rotating rotor. The axis of the rotor is parallel to that of the clinder. The whole system is immersed in a uniform main flow, parallel to the axes of the fuselage and rotor. In the computational model a simplified boundary layer is incorporated. All coordinates and variables are made dimensionless on the (front) rotor tip radius, the speed of sound, and the ambient density of air. Two cylindrical co-ordinate systems will be used in the sequel: one centered on the fuselage axis denoted by $\vec{x} = (x, r, \theta)$, and one centered on the propeller axis denoted by $\vec{x} = (x, r_p, \theta_p)$, see Figure 1. Note that the direction of θ_p has been chosen opposite to that of θ, to be consistent with a positive sense of rotation in a right-handed coordinate system.

In both systems the x-axis is aligned with the main flow $M\vec{\imath}_x$, where M is the flight Mach number. In section III analytical models will be presented for the tonal noise generated by both single rotation rotors (SR) and contra-rotating rotors (CROR). In section IV a model will be presented for the scattering of tones by a cylinder. The final output of the model is the total acoustic pressure of a scattered tone.

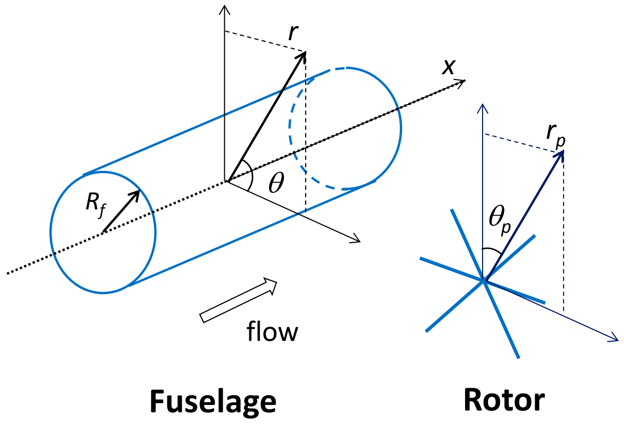

Figure 1 Sketch of fuselage-rotor configuration.

III. Source models

A. Single rotation rotor

In the lifting-line approach the wave equation for the acoustic pressure p and the source term can be written as (Ref. 3):

$$\left[\nabla^2 - \left(\frac{\mathrm{D}}{\mathrm{D}t}\right)^2\right] p = -\sum_{j=0}^{B-1} \nabla_p \cdot \frac{1}{r}\left[\vec{L}(r_p) - \overline{\overline{D}}(r_p)\cdot\nabla\right]\delta(x)\delta(\theta_p - \Omega t - \frac{2\pi j}{B}) \tag{1}$$

with $\frac{\mathrm{D}}{\mathrm{D}t} = \frac{\partial}{\partial t} + M\frac{\partial}{\partial x}$. Here $\vec{L}$ is the force on the blade per unit span, i.e. lift and drag, and $\overline{\overline{D}}$ is a tensor with elements that are proportional to either the pitching moment, also per unit span, or the area of the local cross section of the blade. The latter is responsible for the so-called thickness noise. Furthermore, B is the number of blades and Ω the rotational speed. Ω is positive if the the rotor rotates in clockwise direction, viewed from an upstream position.

In a uniform flow, parallel to the propeller axis, $\vec{L}$ and $\overline{\overline{D}}$ only depend on the radial coordinate and not on the azimuthal position of the blade.

As the pressure field will have the same periodicity as the source, we write the solution as:

$$p(x, r_p, \theta_p, t) = \sum_{n=-\infty}^{\infty} \hat{p}_n(x, r_p) e^{inB(\theta_p - \Omega t)} \tag{2}$$

We take the Fourier transformation in axial direction:

$$\tilde{p}_n(\alpha, r_p) = \int_{-\infty}^{\infty} e^{-i\alpha x}\hat{p}_n(x, r_p)\,\mathrm{d}x \tag{3}$$

which defines α as the axial wavenumber, and find:

$$\left[\frac{\partial^2}{\partial r_p^2}+\frac{1}{r_p}\frac{\partial}{\partial r_p}-\left(\frac{nB}{r_p}\right)^2-\alpha^2+(nB\Omega-M\alpha)^2\right]\tilde{p}_n(\alpha,r_p)$$
$$=\frac{-iB}{2\pi r_p}\left\{\alpha L_x+\frac{nB}{r_p}L_\theta\right.$$
$$\left.-i\left[\alpha^2 D_{xx}+\alpha\frac{nB}{r_p}(D_{x\theta}+D_{\theta x})+\left(\frac{nB}{r_p}\right)^2 D_{\theta\theta}\right]\right\} \tag{4}$$

Here L_x is the component of $\vec{L}$ in x-direction, and similar for L_θ, D_{xx}, etc. A Green's function for the wave operator at the left hand side can be expressed in terms of Bessel functions (J_n) and Hankel functions ($H_n^{(2)}$), (e.g. ref. 4), and we find, transforming back to the x-domain:

$$\hat{p}_n(x,r_p)=\frac{B}{8\pi}\int_{-\infty}^{\infty}e^{i\alpha x}H_{nB}^{(2)}(\gamma r_p)\int_{r_h}^{1}J_{nB}(\gamma\rho)\left\{\alpha L_x+\frac{nB}{\rho}L_\theta\right.$$
$$\left.-i\left[\alpha^2 D_{xx}+\alpha\frac{nB}{\rho}(D_{x\theta}+D_{\theta x})+\left(\frac{nB}{\rho}\right)^2 D_{\theta\theta}\right]\right\}\mathrm{d}\rho\,\mathrm{d}\alpha \tag{5}$$

with $\vec{L}$ and $\overline{\overline{D}}$ evaluated at radial coordinate ρ. The (dimensionless) hub radius is denoted by r_h. Further γ is defined by:

$$\gamma^2=(\omega+M\alpha)^2-\alpha^2, \mathrm{Im}(\gamma)\leq 0 \tag{6}$$

with $\omega=-nB\Omega$.

For the SR tones we adopt a 2[nd] order polynomial distribution of the lift coefficient that has a maximum value of 1 at r = 0.7 and drops to a value of 0.6 at the tip, which gives a distribution that reflects the usual behavior found from computations, see e.g. reference 3. Note that the absolute value is irrelevant in the present context. The direction of the lift is taken to be perpendicular to the local main flow. The contributions from the tensor $\overline{\overline{D}}$ are generally much smaller and not incorporated in the sequel.

B. Contra-rotating rotors

The noise generation mechanism of a CROR is more complicated than that of a single rotor.. The tonal noise consists of rotor-alone tones, which can be described with the same model as for the single-rotation rotor, and of interaction tones for which such a simple model is not available. However, a general expression for these tones can be derived based on the assumption that these tones are generated by the impingement of the viscous wake of the front propeller on the rear blades. In that case the interaction noise can be written as (see ref. 5):

$$p(x,r_p,\theta_p,t)=\sum_{n=-\infty}^{\infty}\sum_{m=-\infty}^{\infty}\hat{p}_{n,m}(x,r_p)e^{i(nB_F-mB_R)\theta_p-i(nB_F\Omega_F-mB_R\Omega_R)t} \tag{7}$$

Here B_F is the number of blades of the front rotor, Ω_F its angular velocity, and the subscript R refers to the rear rotor. We thus find that the solution is a sum over n and m, the terms of which have frequency $\omega=-(nB_F\Omega_F-mB_R\Omega_R)$ and a symmetry pattern with $|nB_F-mB_R|$ lobes. This symmetry pattern rotates with an angular frequency of $\frac{nB_F\Omega_F-mB_R\Omega_R}{nB_F-mB_R}$. The individual tones satisfy:

$$\hat{p}_{n,m}(x,r_p) = \frac{i}{4}\int_{-\infty}^{\infty} e^{i\alpha x} H^{(2)}_{nB_F-mB_R}(\gamma r_p)\int_{r_h}^{1} \rho J_{nB_F-mB_R}(\gamma\rho)\tilde{Q}_{n,m}(\alpha,\rho)\,\mathrm{d}\rho\,\mathrm{d}\alpha \tag{8}$$

No exact model is pursued here for the details of the source, represented by $\tilde{Q}_{n,m}$. In this paper it is assumed that only the unsteady lift on the rear blades, caused by the impingement of the wake of the front propeller, is of interest. As in the sequel of this paper each tone will be analyzed separately, the subscript of $\tilde{Q}$ can be dropped, i.e. the relative magnitude of the tones is not relevant here. In analogy with the expression for the SR propeller, it is assumed that the source can be written as $\tilde{Q} = \left(\alpha q_x + \frac{nB_F-mB_R}{\rho} q_\theta\right)/\rho$, with $\vec{q}$ representing the unsteady lift. As the direction of the unsteady lift will be approximately perpendicular to the local main flow, we take $\frac{q_x}{q_\theta} = \frac{\Omega_R\rho}{M}$. For simplicity we take the magnitude of q constant in ρ, which leads to the final expression:

$$\hat{p}_{n,m}(x,r_p) \approx \frac{iq}{4}\int_{-\infty}^{\infty} e^{i\alpha x} H^{(2)}_{nB_F-mB_R}(\gamma r_p)\int_{r_h}^{1} J_{nB_F-mB_R}(\gamma\rho)\frac{\alpha\Omega_R\rho + \frac{nB_F-mB_R}{\rho}M}{U}\,\mathrm{d}\rho\,\mathrm{d}\alpha \tag{9}$$

with $U(\rho) = \sqrt{(\Omega_R\rho)^2 + M^2}$.

It is clear that this expression does not provide the noise emitted by a CROR in an absolute sense. It is expected however, that the directivity and propagation properties of each tone are described fairly well, as these are mainly governed by (the order of) the Bessel functions. Eq. (9) is therefore suited as a basis for studying the effects of the fuselage and its boundary layer on interaction tones.

IV. Diffraction/refraction by a cylinder and its boundary layer

For the application on the fuselage we switch to the co-ordinate system that is centered on its axis: $\vec{x} = (x, r, \theta)$. In this section a single tone of angular frequency ω is considered. If sources are discarded, the total acoustic pressure amplitude p_{tot} outside the boundary layer satisfies the homogeneous convective wave equation:

$$\left[\nabla^2 - \left(\frac{\mathrm{D}}{\mathrm{D}t}\right)^2\right] p_{tot} e^{i\omega t} = 0 \tag{10}$$

The acoustic field can be written as the sum of an incoming field and a reflected field $p_{tot} = p_{in} + p_{re}$, which each satisfy eq. (10). Eq. (10) is solved by separation in the variables x, r, and θ. After Fourier transformation in circumferential and axial direction the general solution for the reflected field, satisfying the outward radiation condition is:

$$\tilde{p}_{re,n}(\alpha,r) = A_n(\alpha) H_n^{(2)}(\gamma r) \tag{11}$$

Note that this index n is not the same as in the previous sections, where it denoted the n-th harmonic of the propeller BPF. Here it simply denotes the circumferential mode number:

$$p(x,r,\theta) = \sum_{n=-\infty}^{\infty} \hat{p}_n(x,r) e^{in\theta} \tag{12}$$

The meaning of γ is the same as before (eq.(6)).

Inside the boundary layer the Mach number varies as function of r. We assume that the boundary layer is constant in axial direction, which again enables separation of variables. Then we find the following ordinary differential equation for the total amplitude (Ref. 6):

$$\left\{(\omega + M\alpha)\left[\frac{\partial^2}{\partial r^2} + \frac{1}{r}\frac{\partial}{\partial r} - \alpha^2 - \frac{n^2}{r^2} + (\omega + M\alpha)^2\right] - 2\alpha\frac{\partial M}{\partial r}\frac{\partial}{\partial r}\right\}\tilde{p}_{b,n}(\alpha, r) = 0 \tag{13}$$

with boundary condition:

$$\left.\frac{\partial \tilde{p}_{b,n}}{\partial r}\right|_{r=R_f} = 0 \tag{14}$$

and with R_f the radius of the fuselage. Eq. (13) is solved numerically for a function $g(r)$, for each value of α, with boundary condition $g(R_f) = 1$, and $g'(R_f) = 0$. The solution for $\tilde{p}_{b,n}$ can then be written as $B_n(\alpha)g(r)$. By demanding that the total pressure amplitude, and its radial derivative, are continuous at the outside of the boundary layer, the coefficients $A_n(\alpha)$ and $B_n(\alpha)$ can be solved for. Note that eq. (13) is singular at the point where $M(r) = -\frac{\omega}{\alpha}$. This singularity can be treated by approximating the solution near this point with a Frobenius series (ref. 7).

V. Numerical implementation

The relative amplitudes of each mode, as a function of x and θ, are computed by the integration over ρ and α in eqs. (5) and (9). The integration over ρ is done by a simple summation over a number of blade sections, typically about 10. The integration over α is done by using Fast Fourier Transformation (FFT). The axial domain should be large enough so that the amplitudes at both ends are negligibly small. The range in α should at least cover all the propagating contributions, i.e. values for α for which γ is real, see eq. (6). These two conditions set the minimum number of points in x and α. In practice this number is varied between 2^7 and 2^{11}. For simplicity the same number of points is used in the FFT in circumferential direction, eq. (12), in the computation of the scattered field. This is always far more than required, as can be seen by inspection of the modal amplitudes.

For the numerical solution of eq. (13) a 5th order Runge-Kutta solver is used from the Numerical Recipes (ref. 8). The singularity at the point where $M(r) = -\frac{\omega}{\alpha}$ is bridged using a local analytical solution in the form of a Frobenius series (ref. 7).

VI. Cabin noise application: acoustic pressure on the fuselage, with and without BL

In this section results are presented for the tones of a CROR-driven aircraft in cruise conditions. In cruise the acoustic pressure on the fuselage is of great importance as it is the main cause of cabin noise. The parameters used are given in Table 1. The RPM's are selected such that the helical tip speed is still subsonic. The boundary layer is modelled as a 1/7 power law profile, with a thickness of 0.2 m. The coordinate system is chosen such that the propeller axis is at $\theta = 0°$, see Figure 1, and the distance between the propeller and fuselage axes is set at 3.8 m.

Table 1

Altitude	10 km
Mach nr.	0.8
Front rotor tip radius	2 m
Rear rotor tip radius	1.7 m
Fuselage radius	1.5 m
Number of front rotor blades	11
Number of rear rotor blades	8
RPM front	800
RPM rear	940

Figure 2 shows the resulting acoustic pressure on the fuselage for the n=1, m=0 rotor-alone tone, both without (left) and with the boundary layer included (right). In this and following figures the levels are scaled on the maximum value of the incoming pressure on the fuselage. The length of the fuselage section in the computation is 15 meters, which ensures that the levels at the ends are small enough to avoid visible effects from the discrete Fourier transformation.

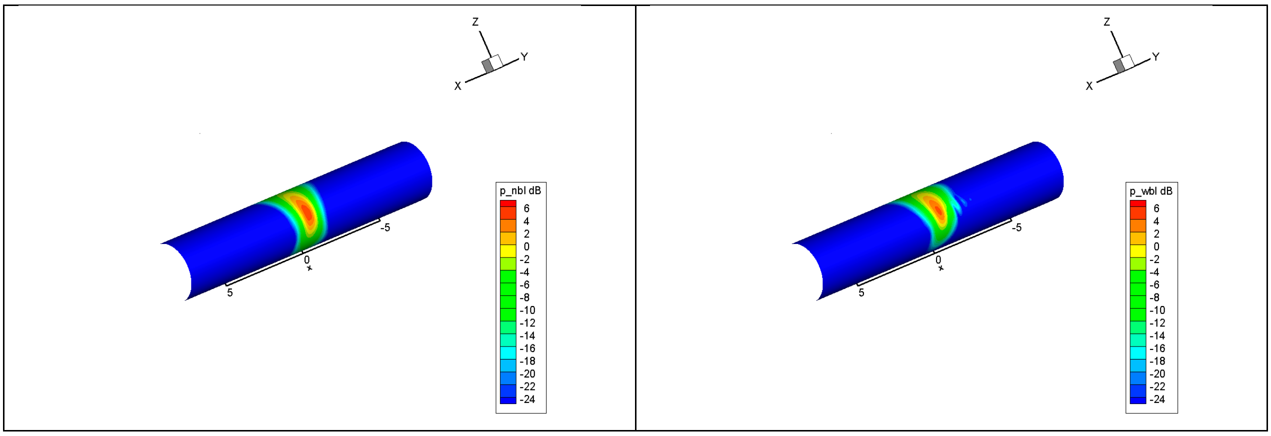

Figure 2 Acoustic pressure levels on the fuselage for the 1,0 rotor-alone tone, without (left) and with the boundary layer included (right).

The reflection by the fuselage without boundary layer causes an increase of the pressure level. The maximum increase in pressure level is 5.3 dB and is concentrated near the propeller plane because the directivity of rotor-alone tones is concentrated in that area. The maximum increase in pressure level is somewhat less than the pressure doubling that would be caused by a flat plate. The pressure increase when the boundary layer is included is smaller, 4.7 dB at maximum. The higher harmonics and the rotor-alone tones generated by the rear propeller show similar behavior and are not shown here.

Figure 3 shows the resulting pressure on the fuselage for the n=1, m=1 interaction tone, both without (left) and with the boundary layer included (right). The source pressure field has been obtained by application of eq. (9), with $q = 1$.

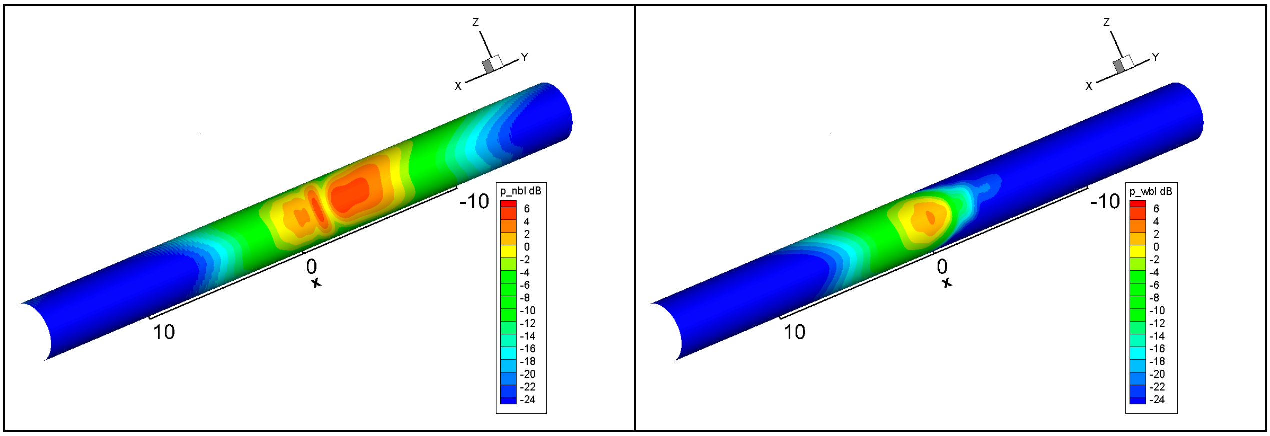

Figure 3 Acoustic pressure levels on the fuselage for the 1,1 interaction tone tone, without (left) and with the boundary layer included (right).

In this case the directivity is much wider than that for a SR tone, which is consistent with test results (see e.g. reference 9) and with the lower order of angular symmetry of the rotor field, $|nB_F - mB_R| = 3$, against $|nB_F - mB_R| = 11$ in the previous case. To avoid spurious effects of the discrete Fourier transform, a longer cylinder has been taken: 34 m. One of the main effects of the boundary layer is that it bends the noise away from the upstream ($x < 0$) part of the fuselage wall, resulting in a significantly lower pressure level. Here the maximum level obtained without boundary layer is 5.7 dB, and with boundary layer 3.0 dB. Note that the effect is not symmetric with respect to the axial position: in downstream direction the noise is bent towards the fuselage which might cause a slight increase of the noise level. This effect is however not visible.

The next example is the n = 2, m = 1 case. The results are shown in Figure 4.

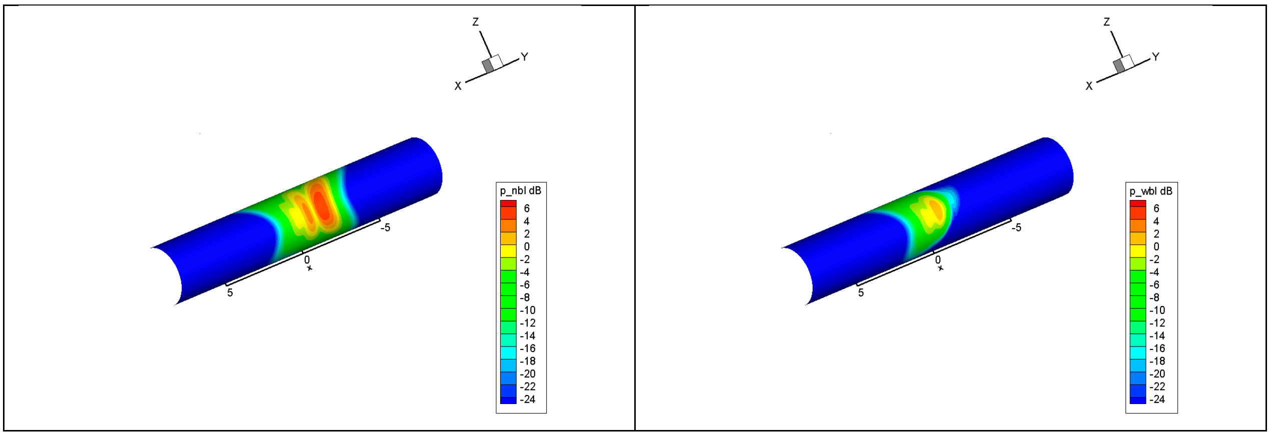

Figure 4 Acoustic pressure levels on the fuselage for the 2,1 interaction tone tone, without (left) and with the boundary layer included (right).

The directivity is more concentrated than in the previous case. This is related to the order of angular symmetry in the rotor field which equals $|nB_F - mB_R| = 14$. The difference in maximum noise levels is quite large here: 5.9 dB (left) against 1.7 dB (right). This might be caused by the higher frequency, 419 Hz against 272 Hz in the previous case. The wavelength is now closer to the thickness of the boundary layer, and the effect of the latter can be expected to be larger.

The final case in this section is the n = 1, m = 2 interaction tone, presented in Figure 5.

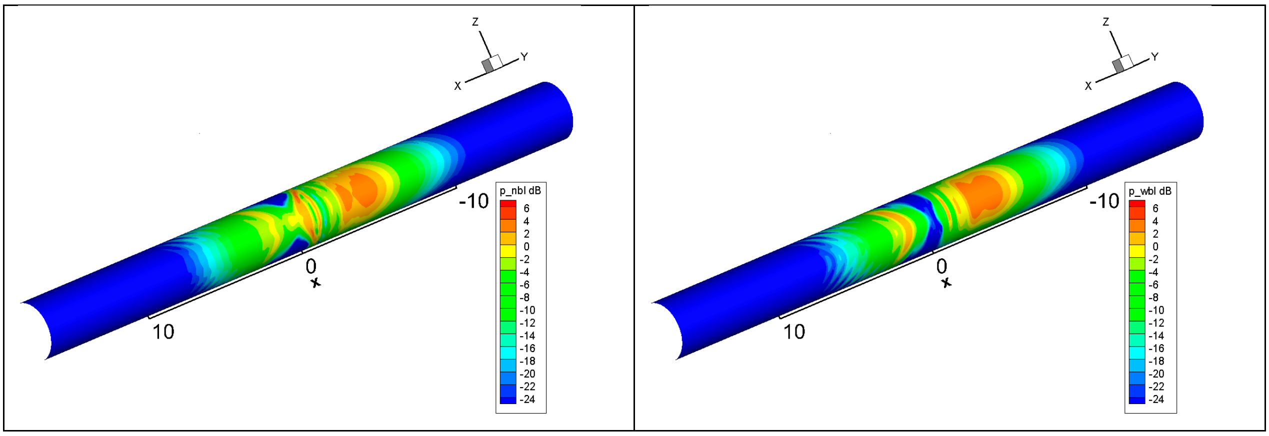

Figure 5 Acoustic pressure levels on the fuselage for the 2,1 interaction tone tone, without (left) and with the boundary layer included (right).

The order of angular symmetry is $|nB_F - mB_R| = 5$, leading to a wider directivity compared to the previous case. The maximum values are now 4.4 dB (left) and 3.9 dB (right).

VII. Results in the Far Field

Far-field results are of interest for community noise, and are therefore computed for a take-off or landing configuration, with a Mach number of 0.2, and zero altitude. As the forward speed is lower, and the speed of sound is higher, a higher rotational speed can be applied, while keeping the helical tip speed subsonic. The parameters used in this section are listed in Table 2.

Table 2

Altitude	0 km
Mach nr.	0.2
Front rotor tip radius	2 m
Rear rotor tip radius	1.7 m
Fuselage radius	1.5 m
Number of front rotor blades	11
Number of rear rotor blades	8
RPM front	1060
RPM rear	1240

The first case considered is again the 1,0 rotor-alone tone. The results are presented in Figure 6. In this case the axial range of the computational domain has been set to -17 < x/R_t < 17, with R_t the tip radius. The plots show the 'shielding factor', i.e. $|p_{tot}/p_{in}|$ as a function of θ, for x = 0 (i.e. in the rotor plane). The blue curves are computed without boundary layer (BL), the red curves are computed with a BL of 0.2 m.

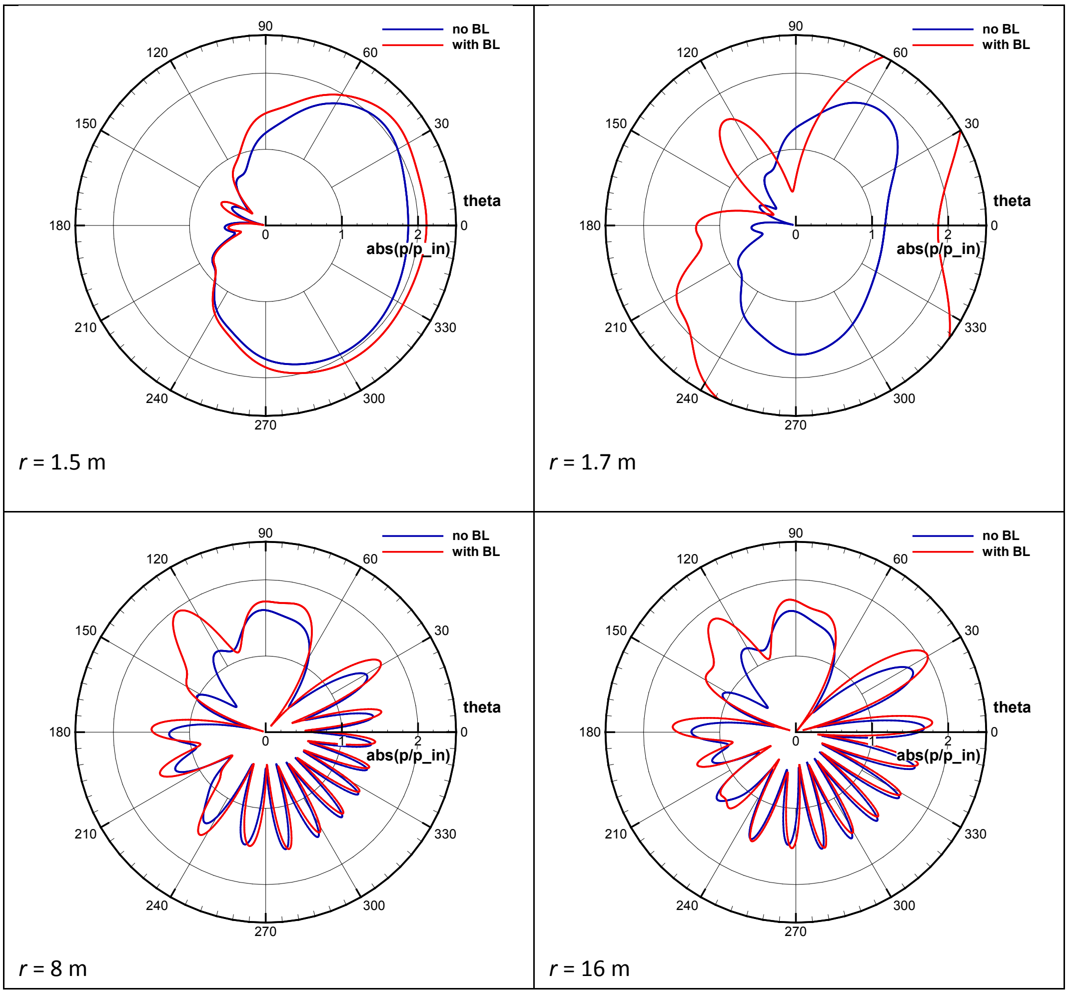

Figure 6 Shielding factor for the 1,0 rotor-alone tone, at x = 0, at 4 different radial distances.

The upper left plot shows the shielding factor on the fuselage. It shows the familiar behavior of approximately a pressure doubling at the rotor side, and strong reductions on the opposite side. The somewhat higher values for the case with BL can be explained by the directivity of the tone: the total pressure is compared to an incoming pressure that is emitted effectively at a different emission angle as the pressure reflected by the fuselage, due to the refraction in the boundary layer. The next figure, for $r = 1.7$ m, shows a similar pattern for the case without BL, but a very deviating curve for the case with BL. This is again due to the effect of directivity mentioned above. At large distances, see the two bottom plots, this effect seems to be much smaller. Moreover, both plots are quite similar, indicating that the far-field limit has almost been reached.

In Figure 7 the SPL is plotted along a sideline, at $\theta = 180°$, i.e. opposite to the rotor, for the two largest radial distances. The levels are scaled to the maximum value of the result for the isolated rotor, the axial distance is scaled to the (front) rotor tip radius. The oscillations, mainly at the left, are caused by the discrete Fourier transform: the pressure is forced to be periodic over the length of the computational domain, about 34 times the tip radius, which introduces (nonphysical) high-wavenumber components.

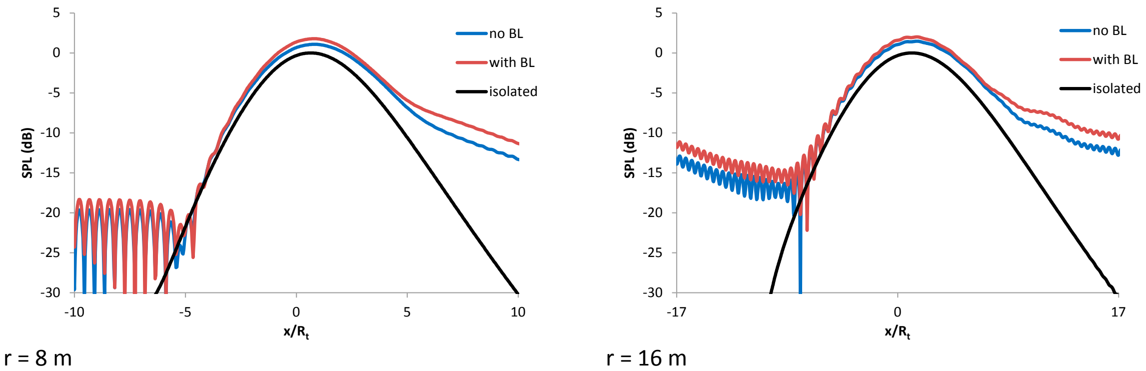

Figure 7 Sideline SPL levels at $\theta = 180°$, for 2 radial distances. 1,0 Rotor-alone tone.

Note that the scales of the x-axis have been adapted such that they have the same ratio as the distance to the propeller axis. The shapes of the curves are then quite similar, again indicating that the far-field limit has been reached.

Next the results for the 1,1 interaction tone are presented, see Figure 8.

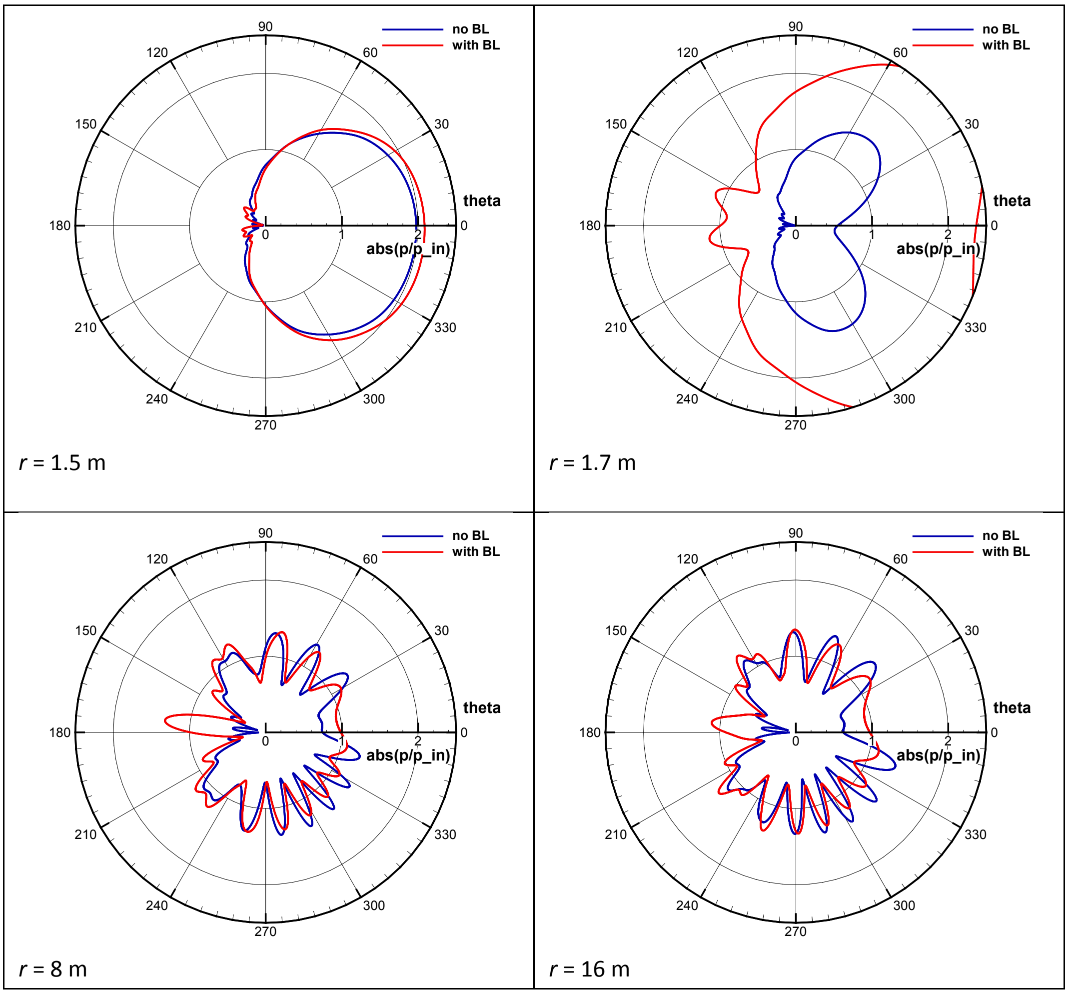

Figure 8 Shielding factor for the 1,1 interaction tone, at *x* = 0, at 4 different radial distances.

In order to obtain meaningful results in the far field, the axial range of the computational domain has been taken much wider than in the previous case: $-45 < x/R_t < 45$. The pressure fields on the fuselage, upper left, again show the familiar diffraction pattern, now for a higher frequency. The results in the far field again show similarity over most of the θ-range, except for the region around $\theta = 180°$ with boundary layer.

In Figure 9 the SPL is plotted along a sideline, at $\theta = 180°$. Again the scales of the *x*-axis have been adapted such that they have the same ratio as the distance to the propeller axis.

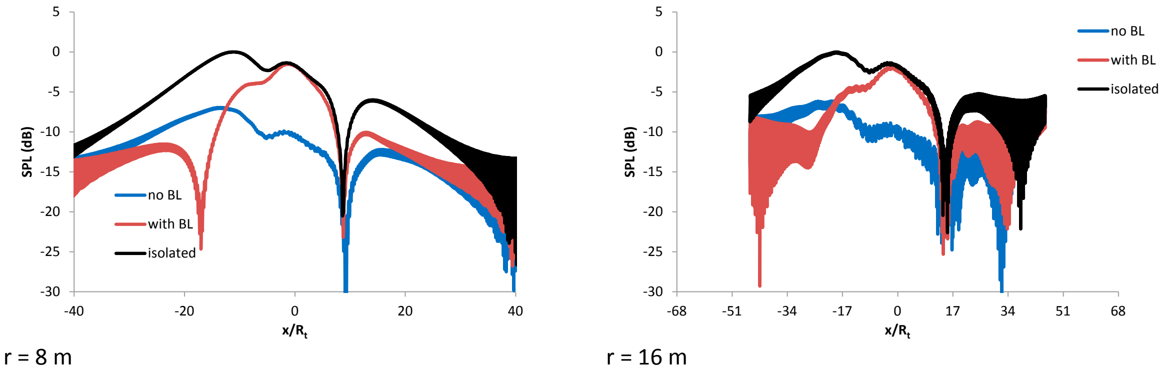

Figure 9 Sideline SPL levels at θ = 180°, for 2 radial distances. 1,1 Interaction tone.

It is clear from these plots why the axial extent of the computational domain has to be taken much larger than in the rotor-alone tone case. Even with this enlarged domain the effects of the discrete Fourier transform are quite severe, due to the fact that at the ends of the domain (i.e. $x/R_t = \pm 45$) the SPL has not decreased yet to a small value. This effect can be reduced by enlarging the domain more and more when looking at larger distances. This will lead to increasing computation times. As an alternative, it is presented in the next section that the issue can be solved by using an analytic far-field approximation.

VIII. Asymptotic far-field approximation

The expressions for the source fields and for the reflected field can all be written in the form:

$$\hat{p}_k(x,r) = \int_{-\infty}^{\infty} e^{i\alpha x} H_k^{(2)}(\gamma r) g(\alpha) \mathrm{d}\alpha \tag{15}$$

see eqs. (5), (9) and (11), where k can be the index in any of these equations. For large values of r we can make use of the asymptotic approximation for the Hankel function, e.g. reference 10:

$$H_k^{(2)}(z) \sim \sqrt{\frac{2}{\pi z}} e^{-i\left(z - \frac{1}{2}k\pi - \frac{1}{4}\pi\right)} \tag{16}$$

If this is substituted into eq. (15) a form is obtained than can be approximated by using the method of stationary phase. The result is:

$$\hat{p}_k(x,r) \sim 2e^{i\left(\frac{\omega R}{\beta}(M\cos\varphi - 1) + \frac{1}{2}\pi(1+k)\right)} \frac{g(\alpha_0)}{\beta R} \tag{17}$$

with:

$$\alpha_0 = \frac{\omega}{\beta^2}(M - \cos\varphi) \tag{18}$$

Here the coordinates R and φ are defined by: $x = \beta R\cos\varphi$ and $r = R\sin\varphi$, with $\beta = \sqrt{1 - M^2}$. This expression shows that at large distances the radiation is dominated by a single axial wavenumber, which depends on the radiation angle in the (x/β, r) plane. To assess this approximation, it is applied to the 1,0 rotor-alone tone. The acoustic pressure amplitudes are computed on a sideline at distances to the fuselage axis of 8 m, 16 m, and 48 m, at

θ = 180°. The results, sound pressure levels and phases, are presented in Figure 10, and compared to results from the 'exact' formulation.

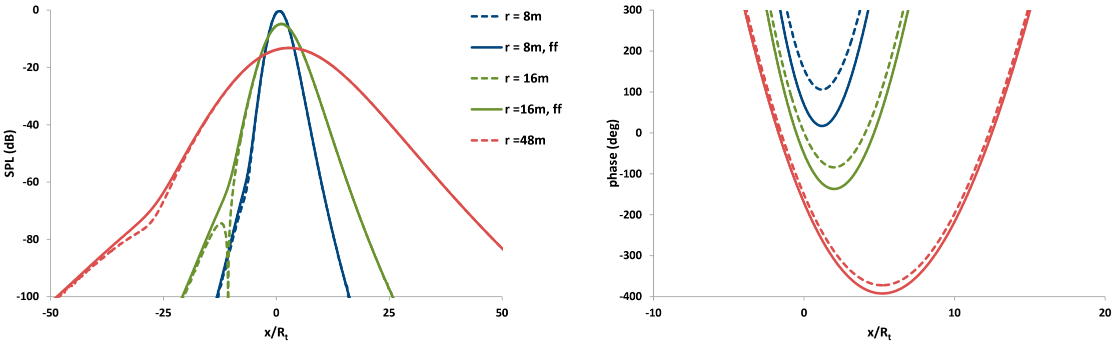

Figure 10 Comparison of 'exact' results with far-field (ff) approximation. Isolated 1,0 rotor-alone tone.

The SPL's are scaled to the maximum level at 8 m. It is remarkable that the SPL's agree very well, even at the short distance of 8m. Only the sharp dip at $x/R_t \approx 10$ in the r = 16 m results is not found in the far-field approximation. The phases however compare less favorably. At r = 8 m the differences are of the order of 70°, decreasing to 50° at r = 16 m, and to 15° at r = 48 m.
Next the same is done for the reflected field, see Figure 11. As in the rest of this section, a boundary layer is not incorporated.

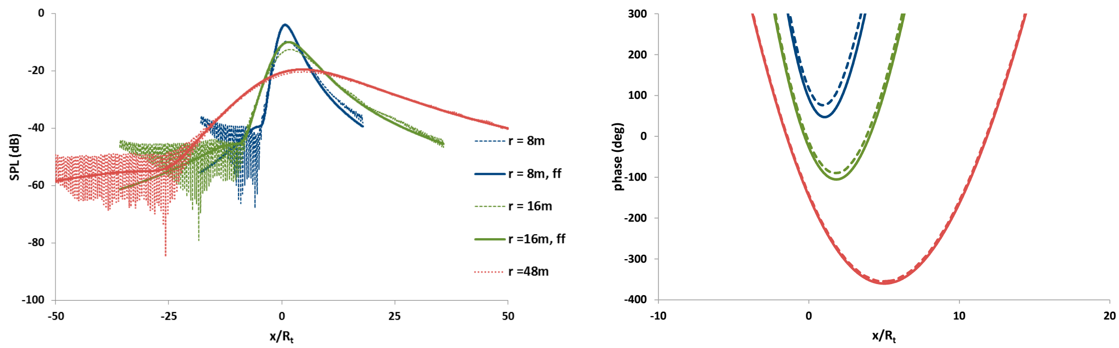

Figure 11 Comparison of 'exact' results with far-field (ff) approximation. Reflected 1,0 rotor-alone tone.

In this case the peak levels at r = 8 m and r= 16 m are somewhat overpredicted by the far-field approximation, but the results for the SPL at r = 48 m agree quite well, apart from the scattering in the 'exact' results caused by the Fourier transformation. The phases differ by typically 30°, 15°, 5° at r = 8 m, 16 m, 48 m respectively.

Both Figures 10 and 11 indicate that the far-field approximation is getting more accurate for larger distances, as may be expected.

To obtain the total acoustic pressure, the results for the isolated pressure and the reflected field have to be added, which only yields correct results if the phases are correct. The result for the total pressure at r =8 m and r = 16 m can therefore not be expected to be accurate in the far-field approximation. In the next figure the directivity pattern of the shielding factor is plotted for r =16 m and r = 48 m.

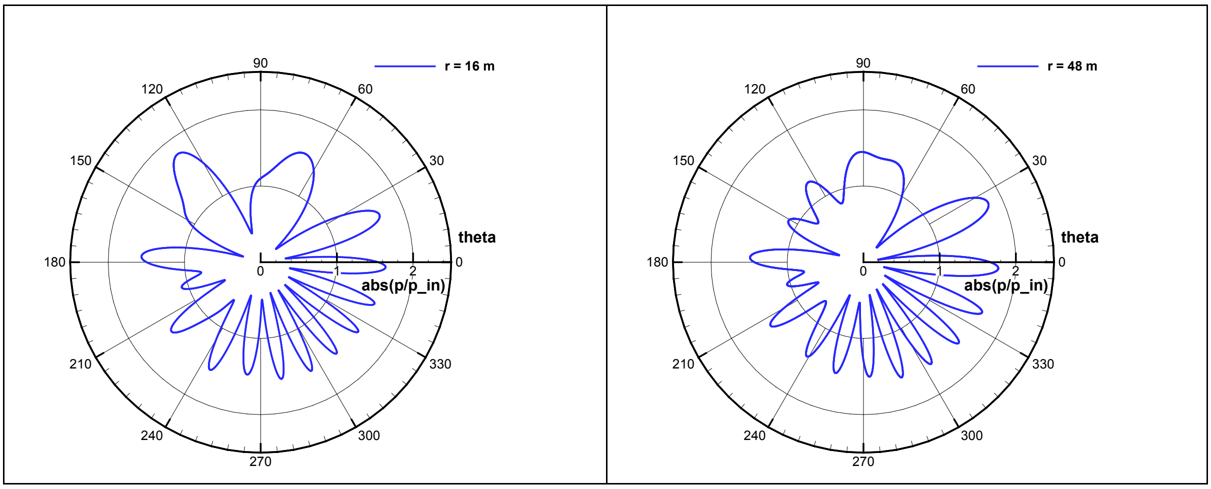

Figure 12 Shielding factor for the 1,0 rotor-alone tone at x = 0 at two radial distances, far-field approximation.

Indeed, the left hand plot shows large differences compared to the two lower plots in Figure 6 (no BL), especially in the range from θ = 30° to 180°. The right hand plot however agrees better with Figure 6, which indicates that the distance of 48 m is large enough to obtain good results from the far-field approximation. In Figure 13 the sideline SPL levels are shown of the isolated and the total pressure field at r = 48 m, both from the far-field approximation. The shape compares quite well to the plots in Figure 7, but here the curves are not distorted by the effects of the discrete Fourier transformation.

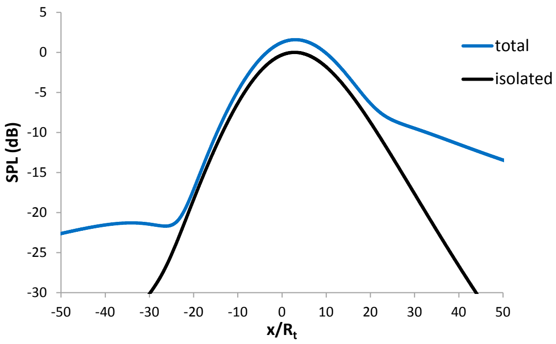

Figure 13 Sideline SPL levels at θ = 180°, r = 48 m. 1,0 Rotor-alone tone, far-field approximation.

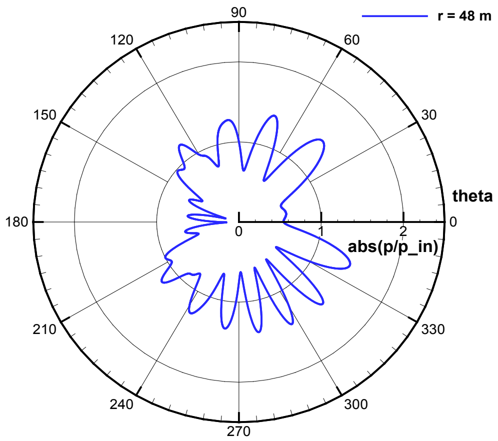

Figure 14 Shielding factor for the 1,1 interaction tone at $x = 0$ at $r = 48$ m, far-field approximation.

Finally, results from the far-field approximation are presented for the 1,1 interaction tone. In Figure 14 the directivity pattern of the shielding factor is plotted for $r = 48$ m. This plot resembles the plots (bottom row, no BL) of Figure 8. The sideline SPL's at r =48 are shown in Figure 15 (left hand side). Some ripples are visible, due to the small error in the phases in the far-field approximation. Apart from that, the curves are much smoother than those of Figure 9. The relative level of the total pressure is somewhat higher than in Figure 9, which may also be ascribed to the error in the phases.

To check this, the same data have also been computed for a radial distance of 1000m, see Figure 15 (right hand side). The ripples are still there, but the relative levels of the total pressure are now more in agreement with those of Figure 9.

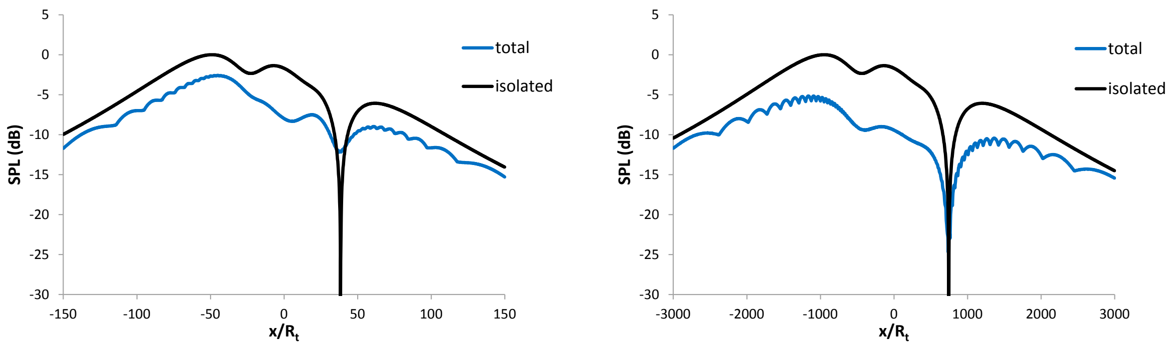

Figure 15 Sideline SPL levels at θ = 180°, r = 48 m (left) and r = 1000 m (right). 1,1 Interaction tone, far-field approximation.

IX. Conclusions

A model is presented for the computation of the acoustic interaction of open rotors and a rigid cylinder, representing an aircraft fuselage. An analytic description of the rotor noise sources is used that is quite accurate in the case of a single-rotation propeller, and contains the main spatial characteristics of the sound field in the case of a contra-rotating open rotor (CROR). In the computation of the sound field of an installed configuration the boundary layer can be incorporated. The model is suitable for computing both the acoustic pressure on the fuselage wall, relevant for cabin environment studies, and the pressure waves radiated to the far-field.

In the first application it is shown that the boundary layer significantly decreases the pressure level on the fuselage upstream of the rotor. This is caused by the gradient of the velocity profile in the boundary layer, which bends the acoustic waves away from the fuselage wall. Results are presented for a rotor-alone tone and a few interaction tones.

Results for the scattered acoustic field are also presented at some distance from the fuselage. Directivity plots show interference patterns with a strong variation of the sound pressure level as a function of circumferential angle. At larger distances the results are distorted by the discrete Fourier applied in axial direction. This effect forces the use of a large computational domain in axial direction, especially in the case of interaction tones, which radiate over a wider angular range than rotor-alone tones. As an alternative, an asymptotic approximation is derived for large distances, avoiding the discrete Fourier transformation. This method results into smooth curves at low computational costs. However, care should be taken with respect to the range of application; at intermediate distances the far-field approximation leads to significant errors in the computed phase and the results are not suitable for the computation of interference patterns.

The analytic formulations presented in this paper provide a powerful tool to estimate the effect of a fuselage and it boundary layer on rotor noise, both as it impinges on the fuselage itself and as it radiates to the far field. The effort to prepare the computations and the computational costs are very low. Although the method is not suitable to predict installed rotor noise accurately for a real aircraft geometry, it can be used to better understand the effects, to yield a quick first estimate of the installation effects, and to serve as a benchmark for high-fidelity computational methods.

References

[1]McAlpine, A. and Kingan, M.J., “Far-field sound radiation due to an installed open rotor”, *International Journal of Aeroacoustics*, Vol. 11, nr.2, pp. 213-245, 2012.

[2]Kingan, M.J. and Self, R.H., “Open rotor tone scattering”, *J. Sound Vib*., Vol. 331, pp. 1806-1828, 2012.

[3]Brouwer, H.H., “On the use of matched asymptotic expansions in propeller aerodynamics and acoustics”, *J. Fluid Mech.*, Vol.242, pp.117-143, 1992.

[4]Schulten, J.B.H.M., “Sound Generation by Ducted Fans and Propellers As a Lifting Surface Problem.”, PhD Thesis, Twente University, 1993.

[5]Brouwer, H.H., “Analytic description of the noise radiation from single- and contra-rotating propellers”, *27th Congress of the International Council of the Aeronautical Sciences (ICAS)*, 19 - 24 September 2010, Nice, France, paper 105, 2010.

[6]Goldstein, M.E., “Aeroacoustics”, McGraw-Hill, 1976.

[7]Hanson, D.B., and Magliozzi, B., “Propagation of Propeller Tone Noise Through a Fuselage Boundary Layer”, *J. Aircraft*, vol. 22, no. 1, January 1985.

[8]Press, W.H., Teukolsky, S.A., Vetterling, W.T., and Flannery, B.P., *Numerical Recipes in Fortran*, Cambridge University Press, 2nd ed., 1992.

[9]Schnell, R., Yin, J, Funke, S., Siller, H., “Aerodynamic and Basic Acoustic Optimization of a Contra- Rotating Open Rotor with Experimental Verification”, *18th AIAA/CEAS Aeroacoustics Conference*, 04 - 06 June 2012, Colorado Springs, CO, Paper 2012-2127, 2012.

[10]Abramowitz, M. and Stegun, I.A., *Handbook of Mathematical Functions*, National Bureau of Standards, Applied Mathematics Series 55, June 1964, Tenth printing, 1972.

NLR

Anthony Fokkerweg 2
1059 CM Amsterdam, The Netherlands
p) +31 88 511 3113 f) +31 88 511 3210
e) info@nlr.nl i) www.nlr.nl